Hindawi Publishing Corporation
Mathematical Problems in Engineering
Volume 2013, Article ID 712764, 7 pages
http://dx.doi.org/10.1155/2013/712764

Research Article

Design of Magnetic Flux Feedback Controller in Hybrid Suspension System

Wenqing Zhang, Jie Li, Kun Zhang, and Peng Cui

College of Mechatronics Engineering and Automation, National University of Defense Technology, Changsha, Hunan 410073, China

Correspondence should be addressed to Wenqing Zhang; zwq197566@163.com

Received 1 June 2013; Revised 1 September 2013; Accepted 15 September 2013

Academic Editor: Xinkai Chen

Hybrid suspension system with permanent magnet and electromagnet consumes little power consumption and can realize larger suspension gap. But realizing stable suspension of hybrid magnet is a tricky problem in the suspension control sphere. Considering from this point, we take magnetic flux signal as a state variable and put this signal back to suspension control system. So we can get the hybrid suspension mathematical model based on magnetic flux signal feedback. By application of MIMO feedback linearization theory, we can further realize linearization of the hybrid suspension system. And then proportion, integral, differentiation, magnetic flux density B (PIDB) controller is designed. Some hybrid suspension experiments have been done on CMS04 magnetic suspension bogie of National University of Defense Technology (NUDT) in China. The experiments denote that the new hybrid suspension control algorithm based on magnetic flux signal feedback designed in this paper has more advantages than traditional position-current double cascade control algorithm. Obviously, the robustness and stability of hybrid suspension system have been enhanced.

1. Introduction

A hybrid electromagnet made of permanent magnet and electromagnet consumes little power consumption and can realize larger suspension gap. So the hybrid suspension traffic will have more developments in the future. The CMS04 maglev vehicle (Figure 1) designed by National University of Defense Technology (NUDT) has been running above 20 thousand kilometers safely in the national mid-low speed maglev experiment field of Tangshan city in China. Hybrid suspension has high properties of suspension control system; therefore, promoting the robustness and stability of maglev control system is the destination of control engineers. Literature [1] founded the hybrid suspension model based on current feedback. Because the magnetic flux feedback control algorithm has wider control parameters zone and minor overshoot [2], this algorithm has been applied successfully in maglev vehicle of Britain airdrome line. Goodall gives emphasis to the advantages of the magnetic flux signal. Literature [3] mainly designs a robust fuzzy-neural-network control (RFNNC) scheme for the levitated positioning of the linear maglev rail system with nonnegative inputs. A Maglev system is modeled by two self-organizing neural-fuzzy techniques to achieve linear and affine Takagi-Sugeno (T-S) fuzzy systems [4]. The influence of the PID control parameters on the response performance of the system is studied by using the MATLAB SISO [5]. Zhang et al. designed a detailed discourse upon the key technology involved in maglev system, and the method has been carried out in Shanghai maglev traffic on-site, and the results are very significant [6]. Wai and Lee [7, 8] has designed an adaptive fuzzy-neural-network control (AFNNC) scheme by imitating a sliding-mode control (SMC) strategy for a magnetic-levitation (maglev) transportation system. Based on sliding mode control with the feedback linearization, a kind of nonlinear control strategy of electrical Maglev air gap was offered the design method of the system was researched [9]. A nonlinear robust control design for the levitation and propulsion of a magnetic levitation (maglev) system is presented, and a proposed recursive controller is designed using nonlinear state transformation and Lyapunov's direct method in order to guarantee global stability for the nonlinear maglev system [10]. To sum up, the control method based on magnetic flux signal feedback has a bright prospect.

Figure 1: CMS04 maglev vehicle in National mid-low speed maglev experiment field of Tangshan city.

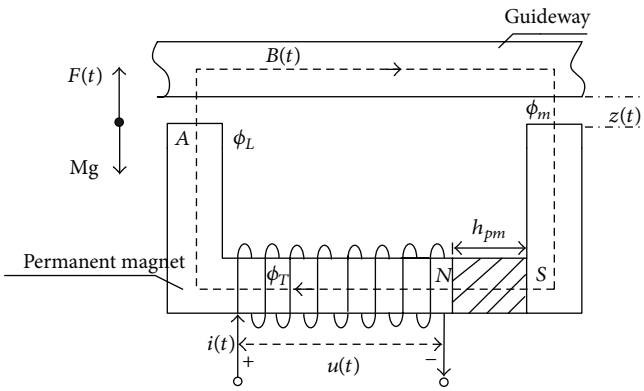

Figure 2: Simple model of hybrid suspension system.

Table 1: Symbols of hybrid suspension system.

Signs	Signification
ϕ_m	Gap flux
ϕ_T	Main flux
ϕ_L	Leaking flux
ψ	Gap flux linkage
$u(t)$	Voltage of magnetic coil
W_m	Magnetic field energy in bulk V
R	Resistance of magnetic coil
B	Gap flux density
μ_0	Magnetic permeability of atmosphere
μ_{pm}	Magnetic permeability of permanent magnet
μ_r	Magnetic permeability of permanent magnet
H_c	Magnetic coercive force of permanent magnet
F_m	Magnetic field potential
R_m	Magnetic resistance
A	Magnetic pole area
$i(t)$	Current of magnetic coil
w_m	Magnetic field energy density
N	Turn of magnetic coil
$z(t)$	Gap in electromagnet and track
F	Electromagnetic force
M	Total quality of suspension object
h_{pm}	Thickness of permanent magnet
g	Acceleration of gravity

2. Modeling of Magnetic Flux Feedback Suspension System

The hybrid suspension system model based on magnetic flux feedback is given in Figure 2.

Illuminating signs of Figure 2 are showing in Table 1.

Assume the following:

(1) magnetic flux formula $\phi_T = \phi_L + \phi_m$, neglect the leaking flux, namely, $\phi_L = 0$,

(2) neglect the magnetic resistance of iron core and the track, assume the magnetic field potential distribute on the suspension gap evenly;

(3) suspension track has infinite rigidity with regard to the electromagnetic, so neglect deformation and the elastic vibration of track.

According to the magnetic ampere theorem, we get magnetic motive force

$$F_m = \oint_L H \cdot dl = Ni + H_c h_{pm}. \tag{1}$$

Calculate the magnetic flux

$$\Phi(z,i) = \frac{F_m}{R_m} = \frac{\mu_0 A\left(Ni + H_c h_{pm}\right)}{2z(t) + h_{pm}/\mu_r}. \tag{2}$$

Magnetic density of position is given by

$$B = \frac{\Phi(z,i)}{A} = \frac{\mu_0\left(Ni + H_c h_{pm}\right)}{2z(t) + h_{pm}/\mu_r}. \tag{3}$$

Magnetic force $F(t)$ at the moment of t is

$$F(t) = \frac{B^2 A}{\mu_0} = \mu_0 A\left[\frac{Ni + H_c h_{pm}}{2z(t) + h_{pm}/\mu_r}\right]^2. \tag{4}$$

From the above equation, we can see that the relation of hybrid magnetic force, current, and position is nonlinear, but the relation between hybrid magnetic force and magnetic density's square is linear, and the hybrid magnetic force is a single function with regard to magnetic flux density.

The electrical dynamic of hybrid suspension system can be treated as an inductance resistance circuit and formulated as follows:

$$\begin{aligned} u(t) &= Ri(t) + \frac{d}{dt}\left[N\Phi(z,i)\right] \\ &= \frac{R}{N\mu_{pm}}\left[B\left(2\mu_r z + h_{pm}\right) - H_c h_{pm}\mu_{pm}\right] + NA\dot{B}. \end{aligned} \tag{5}$$

Transform the above equation

$$\dot{B} = \varphi(x) = \frac{R}{A\mu_{pm}N^2} \cdot \left[H_c h_{pm}\mu_{pm} - x_3 \cdot \left(2\mu_r x_1 + h_{pm}\right)\right] + \frac{1}{NA}u. \tag{6}$$

The hybrid magnetic force can be expressed by

$$M\frac{d^2 z(t)}{dt^2} = Mg + f_d(t) - F(z,i), \tag{7}$$

where f_d is the external disturbance force.

On all accounts above, the mathematical model of hybrid suspension system in Figure 2 can be described as follows:

$$\begin{aligned} B(t) &= \frac{\mu_0\left(Ni(t) + H_c h_{pm}\right)}{2z(t) + h_{pm}/\mu_r}, \\ F(t) &= \frac{B^2(t)A}{\mu_0}, \\ M\ddot{z}(t) &= -F(t) + Mg + f_d(t), \\ u(t) &= \frac{R}{N\mu_{pm}}\left[B(t)\cdot\left(2\mu_r z(t) + h_{pm}\right) - H_c h_{pm}\mu_{pm}\right] + NA\dot{B}(t). \end{aligned} \tag{8}$$

Select state variables

$$x = \begin{bmatrix} x_1 & x_2 & x_3 \end{bmatrix}^T = \begin{bmatrix} z & \dot{z} & B \end{bmatrix}^T. \tag{9}$$

The nonlinear hybrid suspension model is given by

$$\begin{aligned} \dot{x}_1 &= x_2, \\ \dot{x}_2 &= g - \frac{A}{\mu_0 M}x_3^2, \\ \dot{x}_3 &= \frac{R}{A\mu_{pm}N^2}\cdot\left[H_c h_{pm}\mu_{pm} - x_3\cdot\left(2\mu_r x_1 + h_{pm}\right)\right] + \frac{1}{NA}u. \end{aligned} \tag{10}$$

So the nonlinear state space equation is obtained:

$$\begin{aligned} \dot{x} &= f(x) + g(x)u, \\ y &= h(x), \end{aligned} \tag{11}$$

where

$$\begin{aligned} f(x) &= \begin{bmatrix} x_2 \\ g - \dfrac{A}{\mu_0 M}x_3^2 \\ \dfrac{R}{A\mu_{pm}N^2}\cdot\left[H_c h_{pm}\mu_{pm} - x_3\cdot\left(2\mu_r x_1 + h_{pm}\right)\right] \end{bmatrix}, \\ g(x) &= \begin{bmatrix} 0 \\ 0 \\ \dfrac{1}{NA} \end{bmatrix}, \\ h(x) &= x_1, \qquad u = u(t). \end{aligned} \tag{12}$$

The open loop control block diagram of hybrid suspension system is given by Figure 3.

Theorem 1. *The nonlinear system* (4) *and the point* x_0 *existing [9]*

$$\begin{aligned} \dot{x} &= f(x) + g(x)u, \\ y &= h(x). \end{aligned} \tag{13}$$

The necessary and sufficient condition of the accuracy linearization problem at x_0 *[11] is as follows.*

(i) *Rank of* $H = [g, ad_f g, \ldots, ad_f^{n-1} g]$ *is n, and the term n is also the order of the system.*

(ii) *The distribution matrix* $D_{n-1} = \mathrm{span}[g, ad_f g, \ldots, ad_f^{n-1} g]$ *is involution in neighborhood of* x_0.

2.1. Proof the Necessary and Sufficient Condition of Feedback Linearization. Define the equilibrium point $x_0 = [\, z_0 \;\; \dot{z}_0 \;\; B_0 \,]^T$, the terms $z_0 \neq 0$, $\dot{z}_0 = 0$, $B_0 \neq 0$. Compute the vector field $g(x)$, $ad_f g(x)$, and $ad_f^2 g(x)$ generated by the function $f(x)$ and $g(x)$:

$$\begin{aligned} g(x) &= \begin{bmatrix} 0 \\ 0 \\ \dfrac{1}{NA} \end{bmatrix}, \\ ad_f g(x) &= L_f g(x) - L_g f(x) \\ &= \begin{bmatrix} 0 \\ \dfrac{2x_3}{\mu_0 MN} \\ \dfrac{R}{\mu_{pm}A^2N^3}\cdot\left(2\mu_r x_1 + h_{pm}\right) \end{bmatrix}, \\ ad_f^2 g(x) &= [f,[f,g]] \\ &= \frac{\partial\left(ad_f g\right)}{\partial x}\cdot f(x) - \frac{\partial f}{\partial x}\cdot\left(ad_f g\right) \\ &= \begin{bmatrix} -\dfrac{2x_3}{\mu_0 MN} \\ -\dfrac{2R}{AM\mu_0\mu_{pm}N^3}\cdot\left[H_c h_{pm}\mu_{pm} - 2x_3\cdot\left(2\mu_r x_1 + h_{pm}\right)\right] \\ -\dfrac{2R\mu_r}{\mu_{pm}A^2N^3}\cdot x_2 + \dfrac{R^2}{\mu_{pm}^2 A^3 N^5}\cdot\left(2\mu_r x_1 + h_{pm}\right)^2 \end{bmatrix}. \end{aligned} \tag{14}$$

The matrix

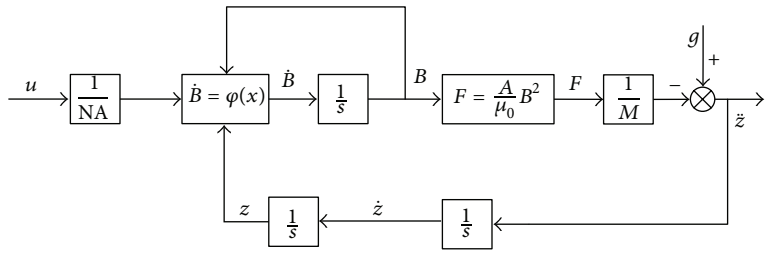

Figure 3: Open loop control block diagram of hybrid suspension system.

$$
\begin{aligned}
H &= \left[g(x), ad_f g(x), ad_f^2 g(x) \right]_{x_0} \\
&= \begin{bmatrix}
0 & 0 & -\dfrac{2x_3}{\mu_0 MN} \\
0 & \dfrac{2x_3}{\mu_0 MN} & -\dfrac{2R}{AM\mu_0\mu_{pm}N^3} \cdot \left[H_c h_{pm}\mu_{pm} - 2x_3 \cdot \left(2\mu_r x_1 + h_{pm} \right) \right] \\
\dfrac{1}{NA} & \dfrac{R}{\mu_{pm}A^2N^3} \cdot \left(2\mu_r x_1 + h_{pm} \right) & -\dfrac{2R\mu_r}{\mu_{pm}A^2N^3} \cdot x_2 + \dfrac{R^2}{\mu_{pm}^2 A^3 N^5} \cdot \left(2\mu_r x_1 + h_{pm} \right)^2
\end{bmatrix}_{x_0} \\
&= \begin{bmatrix}
0 & 0 & -\dfrac{2B_0}{\mu_0 MN} \\
0 & \dfrac{2B_0}{\mu_0 MN} & -\dfrac{2R}{AM\mu_0\mu_{pm}N^3} \cdot \left[H_c h_{pm}\mu_{pm} - 2B_0 \cdot \left(2\mu_r z_0 + h_{pm} \right) \right] \\
\dfrac{1}{NA} & \dfrac{R}{\mu_{pm}A^2N^3} \cdot \left(2\mu_r z_0 + h_{pm} \right) & \dfrac{R^2}{\mu_{pm}^2 A^3 N^5} \cdot \left(2\mu_r z_0 + h_{pm} \right)^2
\end{bmatrix}.
\end{aligned} \tag{15}
$$

Because of $\operatorname{rank}(H) = n = 3$, the terms $g(x_0)$, $ad_f g(x_0)$, $ad_f^2 g(x_0)$ are linearly independent, and also verify that $\operatorname{span}\{g(x), ad_f g(x), ad_f^2 g(x)\}$ is involution distribution in neighborhood of x_0. So the necessary and sufficient condition of the feedback linearization is satisfied.

2.2. Model of Feedback Linearization. Compute the vector field generated by $f(x)$, $g(x)$, and $h(x)$:

$$
\begin{aligned}
L_f^3 h(x) &= -\frac{2R}{AM\mu_0\mu_{pm}N^3} \\
&\quad \cdot \left[H_c h_{pm}\mu_{pm} - 2x_3 \cdot \left(2\mu_r x_1 + h_{pm} \right) \right], \\
L_g L_f^2 h(x) &= -\frac{2x_3}{\mu_0 MN}.
\end{aligned} \tag{16}
$$

Design the feedback controller $u = \alpha(x) + \beta(x)v$, the terms

$$
\begin{aligned}
\alpha(x) &= -\frac{L_f^3 h(x)}{L_g L_f^2 h(x)} \\
&= -\frac{R}{N\mu_{pm}} \cdot \left[H_c h_{pm}\mu_{pm} - x_3 \cdot \left(2\mu_r x_1 + h_{pm} \right) \right], \\
\beta(x) &= \frac{1}{L_g L_f^2 h(x)} = -\frac{\mu_0 MN}{2x_3}.
\end{aligned} \tag{17}
$$

Select the transformation of coordinates

$$
\begin{aligned}
z &= \varphi(x) \\
&= \left[h(x) \;\; L_f h(x) \;\; L_f^2 h(x) \right] = \left[z_1 \;\; z_2 \;\; z_3 \right]^T.
\end{aligned} \tag{18}
$$

Namely, new state variables are obtained as follow:

$$
\begin{aligned}
z &= \left[h(x) \;\; L_f h(x) \;\; L_f^2 h(x) \right]^T \\
&= \left[x_1 \;\; x_2 \;\; g - \frac{A}{\mu_0 M} x_3^2 \right]^T.
\end{aligned} \tag{19}
$$

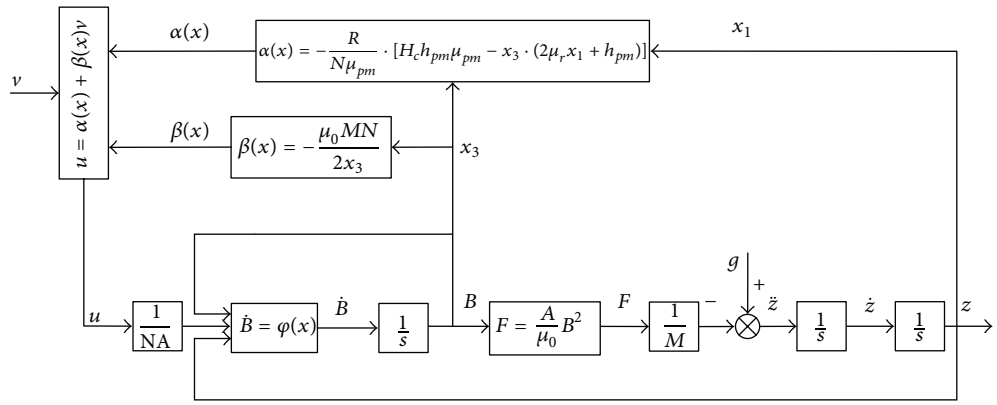

Figure 4: Hybrid suspension system block diagram after linearization.

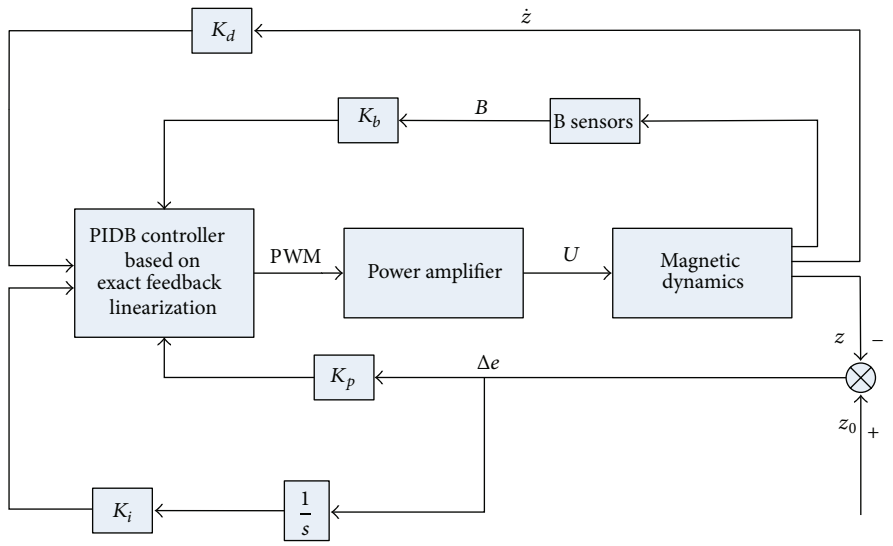

Figure 5: PIDB hybrid suspension control system block diagram based on feedback linearization.

In sum, the hybrid suspension system model after linearization:

$$\dot{z} = \begin{bmatrix} 0 & 1 & 0 \\ 0 & 0 & 1 \\ 0 & 0 & 0 \end{bmatrix} z + \begin{bmatrix} 0 \\ 0 \\ 1 \end{bmatrix} v, \qquad y = \begin{bmatrix} 1 & 0 & 0 \end{bmatrix} z. \tag{20}$$

The maglev system after feedback linearization is a three-level integral system:

$$G_c = \frac{1}{s^3}. \tag{21}$$

The hybrid suspension control block diagram is shown in Figure 4.

3. Design of Maglev Controller

The controlled matrix M_c of linearizing maglev system is

$$\operatorname{rank}\left(M_c\right) = \begin{bmatrix} 0 & 0 & 1 \\ 0 & 1 & 0 \\ 1 & 0 & 0 \end{bmatrix} = 3. \tag{22}$$

Therefore, the hybrid suspension system after linearization is controlled completely, so we can regulate the property of hybrid suspension system by designing PIDB (proportion, integral, differentiation, and magnetic flux density B) suspension controller. Consider

$$v = K_p \cdot (z - z_0) + K_i \cdot \int (z - z_0) \cdot dt + K_d \cdot \dot{z} + K_b \cdot B, \tag{23}$$

where z_0 denotes the given suspension position of hybrid suspension system.

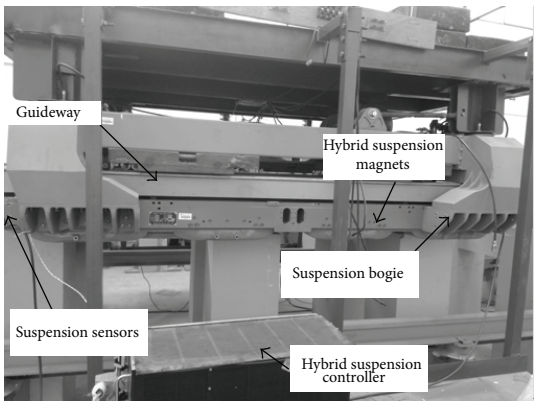

Figure 6: CMS04 hybrid suspension experiment platform.

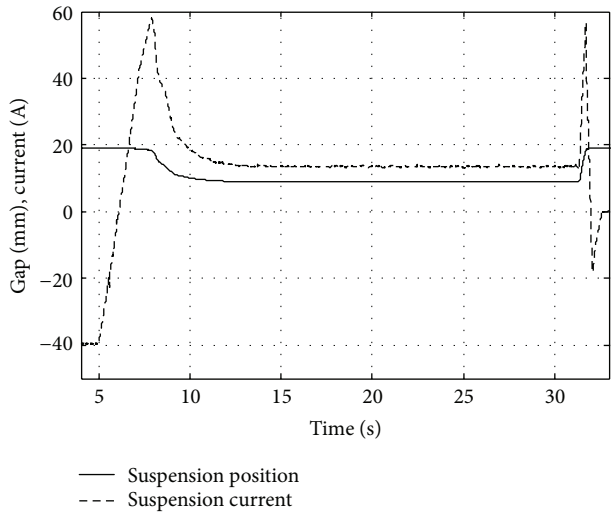

Figure 7: Static suspension process of hybrid suspension system.

Table 2: Hybrid suspension bogie's parameters of CMS04 maglev vehicle.

Parameters	Values
Total mass m [kg]	653
Turn of magnetic coil N [integer]	190
Resistance of magnetic coil R [Ω]	0.5
Magnetic pole area A [m^2]	0.0235
Equilibrium position z_0 [mm]	9
Equilibrium magnetic flux density B_0 [T]	0.6
Equilibrium current i_0 [A]	0
Magnetic permeability of atmosphere μ_0	$4\pi \times 10^{-7}$
Magnetic permeability of permanent magnet μ_r	1.05
Thickness of permanent magnet h_{pm} [mm]	48
Magnetic coercive force of permanent magnet H_c [$kA \cdot m^{-1}$]	880

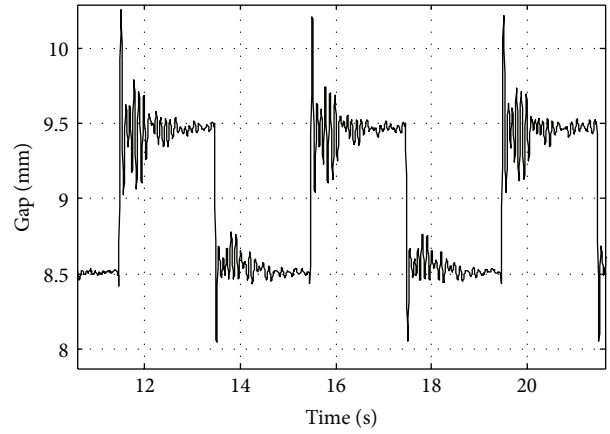

Figure 8: Antijamming property test curves of algorithm S1.

The closed block diagram of hybrid suspension system is as shown in Figure 5.

4. Experiments

The experiment platform is CMS04 hybrid suspension bogie designed by NUDT, showed in Figure 6. Some algorithm experiments have been completed on the standard maglev bogie of the CMS04 maglev vehicle. The first experiment is S1: traditional control algorithm of position-current double cascade control method, and the second is S2: PIDB control algorithm based on state feedback linearization theory designed in this paper. The initial suspension initial position is 25 mm, and the set value is 10 mm. Single standard hybrid suspension bogie's parameters are listed in Table 2.

Experiment 1 (static suspension test). The square quality test on one suspension point of hybrid suspension bogie, setting expected position 9 mm. The experiment applies algorithm S2, and the control parameters are $K_p = 3200$, $K_i = 20$, $K_d = 750$, and $K_b = 260$. The suspension position curve is shown in Figure 7. Suspension process is very stable, so it is proved that PIDB control algorithm is scientific and effective.

Experiment 2 (antijamming property test). The square quality test on one suspension point of hybrid suspension bogie, setting the expect position 9 mm, square amplitude ± 0.5 mm, respectively, applying two control algorithms S1 and S2. The suspension positions are shown in Figures 8 and 9.

The Experiment 2 results denote that the overshoot of S2 is lower obviously than the one of S1. And the Experiment two result indicates that S2 has more robustness, better anti-interference property, and better stability than the ones of S1.

5. Conclusions

According to hybrid suspension physical model, the hybrid magnetic force is a single function with regard to magnetic flux density B. So we take magnetic flux density signal back to maglev control system and design PIDB hybrid suspension control algorithm based on feedback linearization theory. The PIDB control algorithm has been realized on CMS04

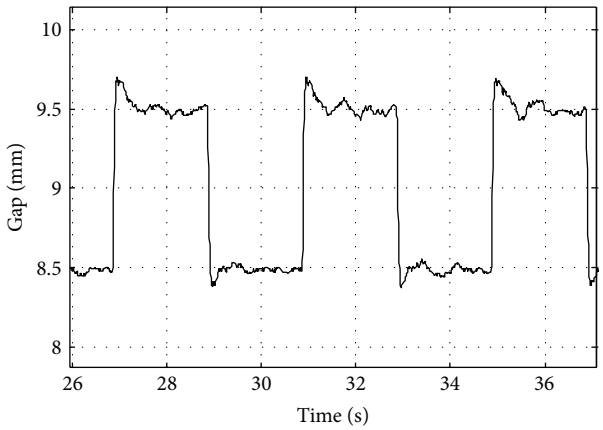

Figure 9: Antijamming property test curves of algorithm S2.

hybrid suspension bogie of NUDT with static suspension test and square property test. The experiments illustrate that new method has stronger antijamming quality than traditional position-current double cascade PID control algorithm.

Acknowledgments

This work was financially supported by National Nature and Science Foundation of China (NNNSFC, nos. 11202230 and 60404003) and the Twelfth Five-year National Science and Technology Support Plan (2012BAC07B01).

References

[1] R. M. Goodall, "Suspension and guidance control system for a dc attraction Maglev vehicle," in *Proceedings of the IEEE Conference*, Publication No 142, pp. 100–103, 1976.

[2] W. Zhang, *Study and realization on suspension control based on magnetic flux feedback [M.S. Dissertation]*, National University of Defense Technology, 2009.

[3] R.-J. Wai and J.-D. Lee, "Robust levitation control for linear Maglev rail system using fuzzy neural network," *IEEE Transactions on Control Systems Technology*, vol. 17, no. 1, pp. 4–14, 2009.

[4] S.-J. Wu, C.-T. Wu, and Y.-C. Chang, "Neural-fuzzy gap control for a current/voltage-controlled 1/4-vehicle MagLev system," *IEEE Transactions on Intelligent Transportation Systems*, vol. 9, no. 1, pp. 122–135, 2008.

[5] D. Liang, S. Fangzhen, and S. Bo, "Parameters optimization and dynamic characteristic analysis of maglev spindle control system," in *Proceedings of the 10th World Congress on Intelligent Control and Automation (WCICA '12)*, pp. 2403–2406, IEEE Conference Publications, 2012.

[6] Z.-J. Zhang, Y. Liu, J.-J. Cheng, and F. Xiong, "Design and research of a new maglev traffic control system," in *Proceedings of the 2nd IEEE International Conference on Advanced Computer Control (ICACC '10)*, pp. 552–556, March 2010.

[7] R.-J. Wai and J.-D. Lee, "Dynamic control of maglev transportation system via adaptive fuzzy-neural-network," in *Proceedings of the International Joint Conference on Neural Networks (IJCNN '07)*, pp. 569–574, August 2007.

[8] R.-J. Wai and J.-D. Lee, "Adaptive fuzzy-neural-network control for maglev transportation system," *IEEE Transactions on Neural Networks*, vol. 19, no. 1, pp. 54–70, 2008.

[9] Z. He and W. Wei, "Study on the sliding mode control system for air gap of electrical Maglev based on the feedback linearization," in *Proceedings of the 7th World Congress on Intelligent Control and Automation (WCICA'08)*, pp. 8003–8007, chn, June 2008.

[10] J. Kaloust, C. Ham, J. Siehling, E. Jongekryg, and Q. Han, "Nonlinear robust control design for levitation and propulsion of a maglev system," *IEE Proceedings—Control Theory and Applications*, vol. 151, no. 4, pp. 460–464, 2004.

[11] C.-K. Chen, C.-J. Lin, and L.-C. Yao, "Input-state linearization of a rotary inverted pendulum," *Asian Journal of Control*, vol. 6, no. 1, pp. 130–135, 2004.